Chapter 6

A Novel Discotic Mesogenic Dimer TpImTp and its Complex with DNA at Interfaces

6.1 Introduction

The discotic molecule comprising more than one aromatic core are referred to as "discotic oligomers". They represent a very attractive class of discotic mesogens since, in general, they demonstrate a higher degree of order compared to their "monomeric" analogs [1]. Among the discotic oligomers, those which contain two discotic groups linked via a flexible spacer (or a rigid spacer) are called "discotic dimers". These dimers represent ideal model compounds for polymers or networks [2, 3]. The physical properties of the dimers are significantly different from the conventional low molar mass discogens because of restricted molecular motions [4]. The widely studied systems in this regard are the HBC (hexa-*peri*-hexabenzocoronene) derivatives. The HBC monomer forms a well defined columnar mesophase. When two HBC units are directly linked to form a dimer, the columnar self-organization is not possible due to intermolecular torsion. On the contrary, a dimer with two HBC units connected by a sufficiently long and flexible spacer shows mesophase behavior slightly different from the HBC monomer [5]. Further, seven HBC units linked together forming a star-like shape shows a well ordered hexagonal columnar mesophase, which exhibits a rare case of gelation exclusively due to π-π interaction [6]. There are also examples of other discotic oligomers known in the literature which form various columnar mesophases and sometimes exhibit very complex phase behavior [7, 8].

Although there are plenty of studies on discotic oligomers in the bulk, there are only a few studies on the organization of such molecules at the air-water (A-W) interface. Maliszewskyj et

al. have reported stable Langmuir monolayer formation of a star-shaped discotic oligomer with mesogenic triphenylene subunits [9]. At the A-W interface, the oligomer molecules exhibited a conformation such that the peripheral triphenylene subunits sit perpendicular to, and the central core sits parallel to, the interface. In addition, their atomic force microscope (AFM) measurements indicated that the conformation of the molecules was preserved upon transfer to a solid substrate. Also, the triphenylene subunits of these molecules were organized in columns with average alignment along the direction of deposition [9]. Tsukruk et al. have reported LB films of discotic dimer and trimer molecules composed of chemically connected donor (triphenylene) and acceptor (trinitrofluorenone) subunits [10]. They observed macroscopic imperfections represented by micron size fractures and ruptures in the LB films. In another report, it was shown that a smooth and perfect LB film can be obtained by attaching the discotic triphenylene group to a polymer backbone [11].

In Chapter 2, we have presented the stable Langmuir monolayer formation of an imidazolium-based triphenylene (ImTp) molecule which was a monomer. The formation of supramolecular assemblies containing imidazolium-based discogens may find applications as heat carriers in solar-thermal energy generators and as electrolytes for batteries and capacitors [12, 13]. Although some imidazolium-based discotic mesogens are known [14], the dimers of such molecules have not yet been explored in literature. Hybridization of two triphenylene cores with an imidazolium moiety to form dimer may lead to novel material with interesting properties.

In this chapter, we present the studies on the films of a novel ionic discotic dimer consisting of two triphenylene cores linked via alkyl spacer with a imidazolium moiety (TpImTP). The TpImTp dimer forms a stable monolayer at the A-W interface with a limiting area and compressional elastic modulus much greater than that of its monomer analog (i.e., the ImTp molecule) [15]. In addition, we have formed TpImTp-DNA complex at the A-W interface by adding DNA in the ultrapure water subphase. We have formed LB films of both the pure TpImTp and the TpImTp-DNA complex. For a comparison with its monomer analog, we have also formed the monomer ImTp-DNA complex monolayer at the A-W interface.

6.2 Experiment

The material TpImTp was synthesized by Santanu Kumar Pal and Sandeep Kumar [16]. The compound was purified by repeated recrystallizations with diethyl ether and characterized by ^{1}H NMR, ^{13}C NMR, IR, UV spectroscopy and elemental analysis which indicated high purity (99%) of the material. The thermotropic liquid crystalline properties of this compound was investigated by polarizing optical microscopy and differential scanning calorimetry. The surface manometry and BAM experiments were carried out at the A-W interface. For the complex formation with DNA, sodium salts of deoxyribonucleic acid was dissolved in the ultrapure water subphase. This is a double stranded DNA with approximate molecular weight of 1.3×10^{6} and about 2000 base pair (Sigma). Atomic force microscope (AFM) studies were performed on the Langmuir-Blodgett (LB) films of both the pure and complex systems on silicon substrates. The hydrophilic and hydrophobic silicon substrates were used for the LB film deposition. The methods of the substrate preparation are presented in Chapter 2. For the AFM studies, we have used silicon tips with a spring constant of 21 N/m and resonance frequency of 250 kHz. The AFM images were obtained using the AC mode in ambient conditions. All the experiments were carried out at room temperature (~25 °C). The details of the experimental techniques are presented in Chapter1.

6.3 Results

The material TpImTp in the bulk exhibits the following phase sequence: Solid − columnar phase (Col); 84°C, Col − isotropic; 95°C. On cooling, the columnar mesophase appeared at 92°C and remained stable down to room temperature. The structure of the columnar mesophase obtained by small angle XRD revealed a simple rectangular lattice of parameter a = 3.48 nm and b = 3.03 nm [16].

6.3.1 Surface Manometry

The surface pressure (π) - area per molecule (A_m) isotherm for TpImTp monolayer on ultrapure water subphase is shown in Figure 6.1. The isotherm shows single phase with a limiting area (A_o) value of 1.97 nm^2/molecule. The A_o value was obtained by extrapolating the slope of the

steep region of the isotherm to zero surface pressure (shown by the red line in Figure 6.1). The monolayer collapses at an A_m of 1.5 nm^2/molecule with a collapse pressure of about 39 mN/m.

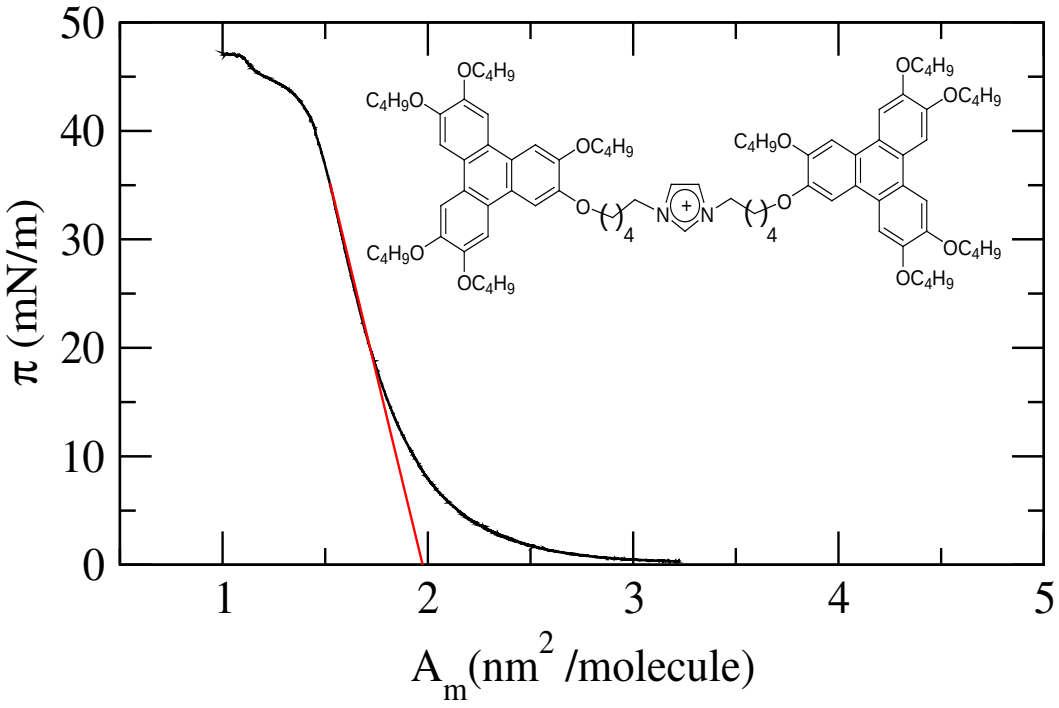

Figure 6.1: The surface pressure (π) - area per molecule (A_m) isotherm of TpImTp monolayer on ultrapure water subphase. The extrapolation of the slope at the steep region of the isotherm to zero surface pressure shown by the red line gives the value of limiting area per molecule (A_o) to be 1.97 nm^2/molecule.

The isotherm cycles were performed by expanding and compressing the monolayer film at the air-water interface. Figure 6.2 shows the π - A_m isotherm cycles of TpImTp monolayer. Similar to the discotic monomers, this film also showed reversibility from the collapsed state to the monolayer state with negligible hysteresis.

We have studied the interaction of the TpImTp monolayer with DNA. We find that with the increase in concentration of DNA in the subphase, the limiting area of the isotherm decreases and the collapse pressure increases. However, beyond 10^{-8} M concentration of DNA in the subphase, there was no further change in the isotherm. Figure 6.3 shows the π-A_m isotherm of TpImTp-DNA complex monolayer with 10^{-8} M concentration of DNA in the subphase. At this concentration, the isotherm exhibited a slope change around 1.6 nm^2/molecule indicating a phase transformation. The limiting area corresponding to the gradual rise region was 2.2 nm^2/molecule and steep rise

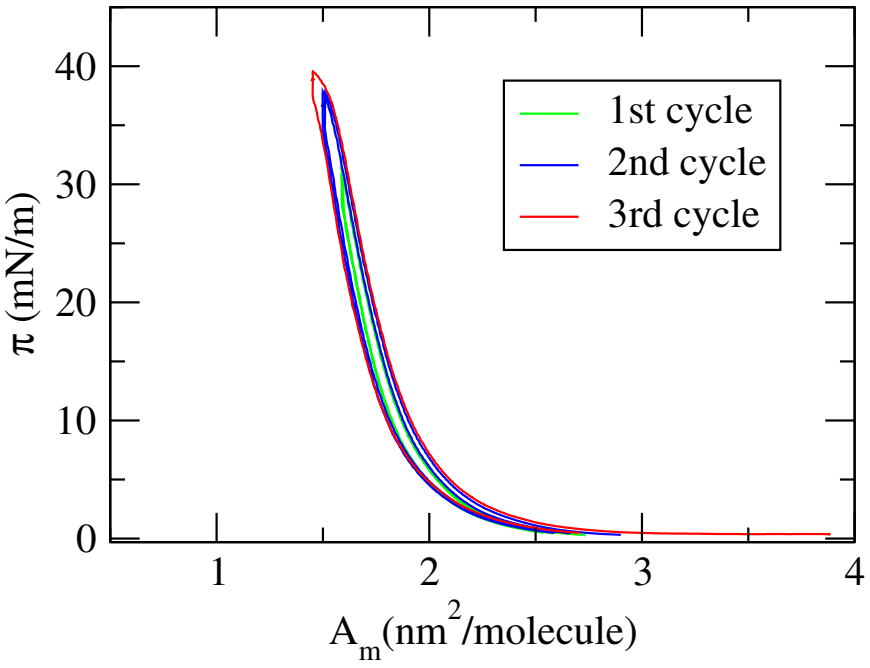

Figure 6.2: The π - A_m isotherm cycles of TpImTp monolayer at the air-water interface showing reversibility from the collapsed state to the monolayer state with negligible hysteresis.

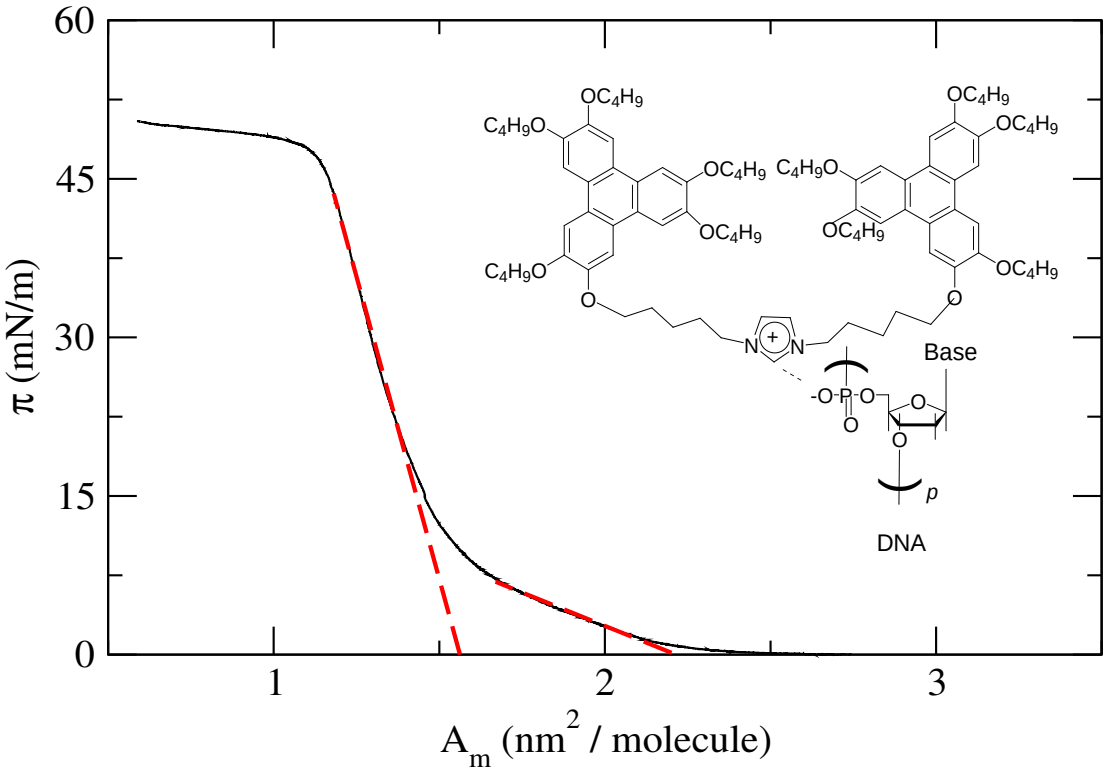

Figure 6.3: The π-A_m isotherm of the TpImTp-DNA complex monolayer with 10^{-8} M concentration of DNA in the subphase.

region was 1.56 nm^2/molecule. The complex monolayer collapsed at an A_m of 1.2 nm^2/molecule with a collapse pressure of 47 mN/m.

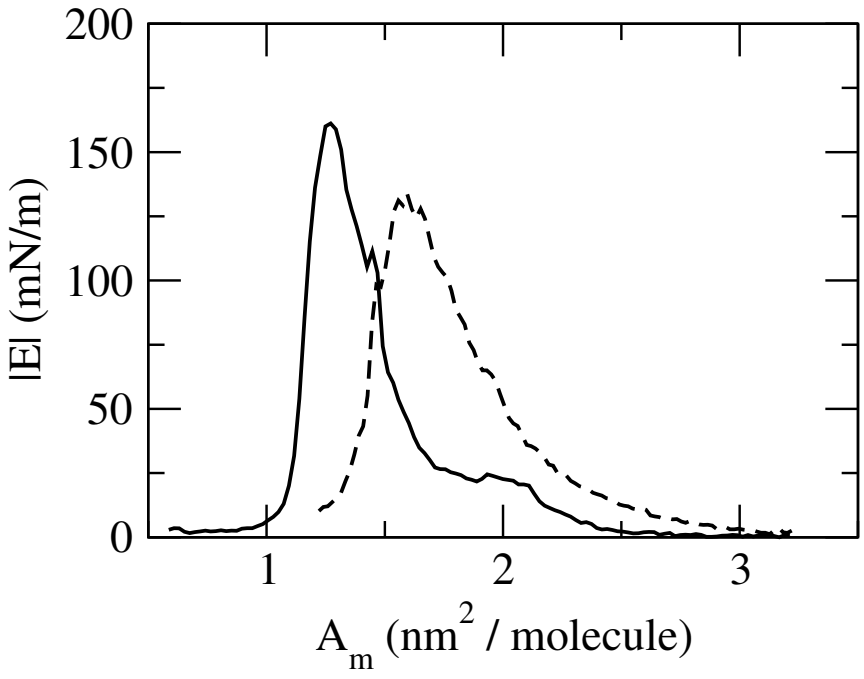

Figure 6.4: Variation of compressional elastic modulus (|E|) with area per molecule (A_m) for the TpImTp monolayer (dashed line) and the TpImTp-DNA complex monolayer (solid line) at the air-water interface.

We have calculated the compressional elastic modulus |E| from the isotherms of both the pure TpImTp monolayer and the TpImTp-DNA complex monolayer. |E| is given by $A_m(d\pi/dA_m)$, where $d\pi/dA_m$ is the change in surface pressure with area per molecule [17]. Figure 6.4 shows the variation of |E| with A_m for the pure TpImTp monolayer and the TpImTp-DNA complex monolayer with 10^{-8} M concentration of DNA in the subphase. The $|E|$ value showed a maximum of 132.3 mN/m at A_m of 1.56 nm^2/molecule for the pure TpImTp monolayer. The maximum value of $|E|$ for TpImTp-DNA complex was 163 mN/m at A_m of 1.26 nm^2/molecule. In addition, the $|E|$ versus A_m curve showed a hump at 1.94 nm^2/molecule with a value of 24.0 mN/m for the TpImTp-DNA complex monolayer.

It is known that the properties exhibited by a dimer molecule is different from those exhibited by its monomer analog [2]. Therefore, we have also carried out similar surface manometry studies for the monomer analog i.e., ImTp molecule. In Chapter 2, we presented the surface manometry

studies of the pure ImTp molecule. Here, we present the studies on ImTp-DNA complex monolayer. Figure 6.5 shows the π-A_m isotherms of the monomer ImTp molecule with 10^{-7} M and 10^{-8} M concentrations of DNA in the subphase. The variation in $|E|$ value with A_m is also shown in Figure 6.5. The isotherms show A_o values of 1.73 nm^2/molecule for the gradual rise region and 1.11 nm^2/molecule for the steep rise region. We find a maximum of 98 mN/m in the $|E|$ value of the ImTp-DNA complex monolayer. Additionally, we find a hump with a value of 24.3 mN/m in the $|E|$ curve corresponding to the gradual rise region of the isotherm of ImTp-DNA complex monolayer.

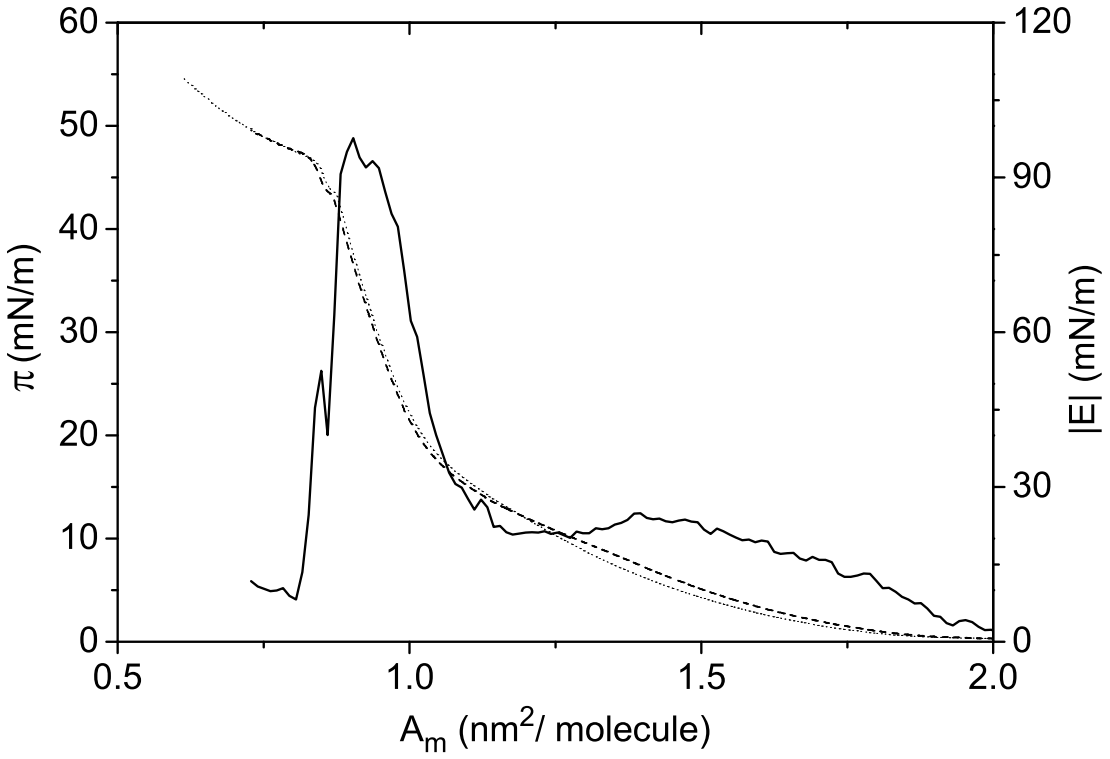

Figure 6.5: The surface pressure (π) - area per molecule (A_m) isotherms of ImTp molecule with 10^{-7} M (dotted line) and 10^{-8} M (dashed line) concentrations of DNA in the subphase. The variation of compressional elastic modulus (|E|) with A_m is shown by the continuous line. The |E| values were same for both the isotherms with 10^{-7} M and 10^{-8} M concentrations of DNA in the subphase.

6.3.2 Brewster Angle Microscopy

The TpImTp monolayer and the TpImTp-DNA complex monolayer films were observed under BAM while compressing the respective monolayers. Figure 6.6 shows the BAM images for the pure TpImTp monolayer. The film exhibited a uniform phase from nearly zero surface pressure. The brightness gradually increased upon compressing the film indicating a uniform condensed phase (Figure 6.6(a)). This uniform phase transformed to three-dimensional (3D) crystals at the collapse state (Figures 6.6(b) and 6.6(c)). On expansion, these crystalline domains disappeared and the system reverted back to the uniform intensity region indicating a monolayer state.

The BAM images for the TpImTp-DNA complex monolayer are shown in Figure 6.7. At large A_m, the complex film exhibited a coexistence of gas and expanded phase (Figure 6.7(a)). This transformed to a uniform expanded phase upon compression (Figure 6.7(b)). At an A_m of about 1.4 nm^2/molecule, a condensed phase was found to develop over the expanded phase (Figure 6.7(c)). Upon further compression, the film transformed to a uniform condensed phase (Figure 6.7(d)). When the film was still compressed, thread-like 3D domains appeared at the collapsed state (Figure 6.7(e)). On expanding the film, these thread-like 3D domains remained without change and the film did not revert back to the monolayer state.

In addition, the monomer ImTp-DNA complex monolayer film was observed under BAM during compression. The features observed were similar to that of the TpImTp-DNA complex film. At large A_m, the ImTp-DNA complex film showed a coexistence of gas and expanded phase which transformed to a uniform expanded phase upon compression. On further compression, the monolayer transformed to the coexistence of expanded and condensed phase, and then to a uniform condensed phase. Compressing still further, the monolayer transformed to a collapsed state. At the collapsed state, the ImTp-DNA film showed thread-like 3D domains similar to that of the collapsed domains of the TpImTp-DNA complex film. On expansion, these thread-like collapsed domains remained without change indicating that the ImTp-DNA complex film did not revert back to its monolayer state.

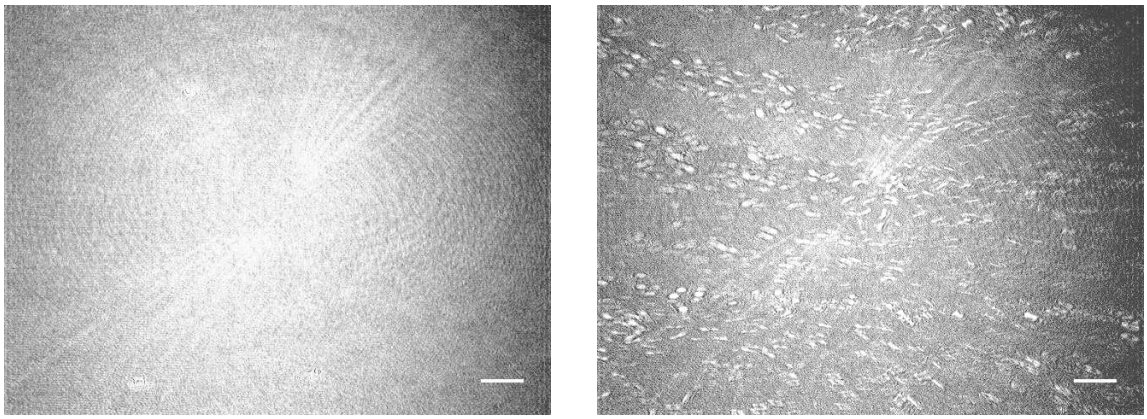

(a) (b)

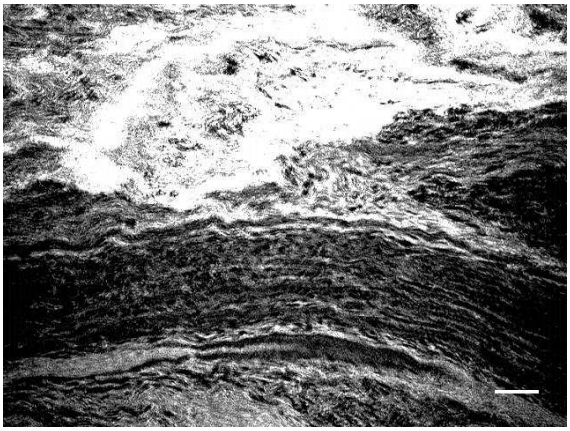

(c)

Figure 6.6: Brewster angle microscope images taken during compression of the TpImTp monolayer film at the air-water interface. (a) Uniform bright intensity indicating a condensed phase at A_m = 1.50 nm^2/molecule. (b) 3D crystals developing over condensed phase indicating the onset of collapse state at A_m = 1.20 nm^2/molecule. (c) Collapsed state at A_m = 0.70 nm^2/molecule. The scale bar in each image represents 500 μm.

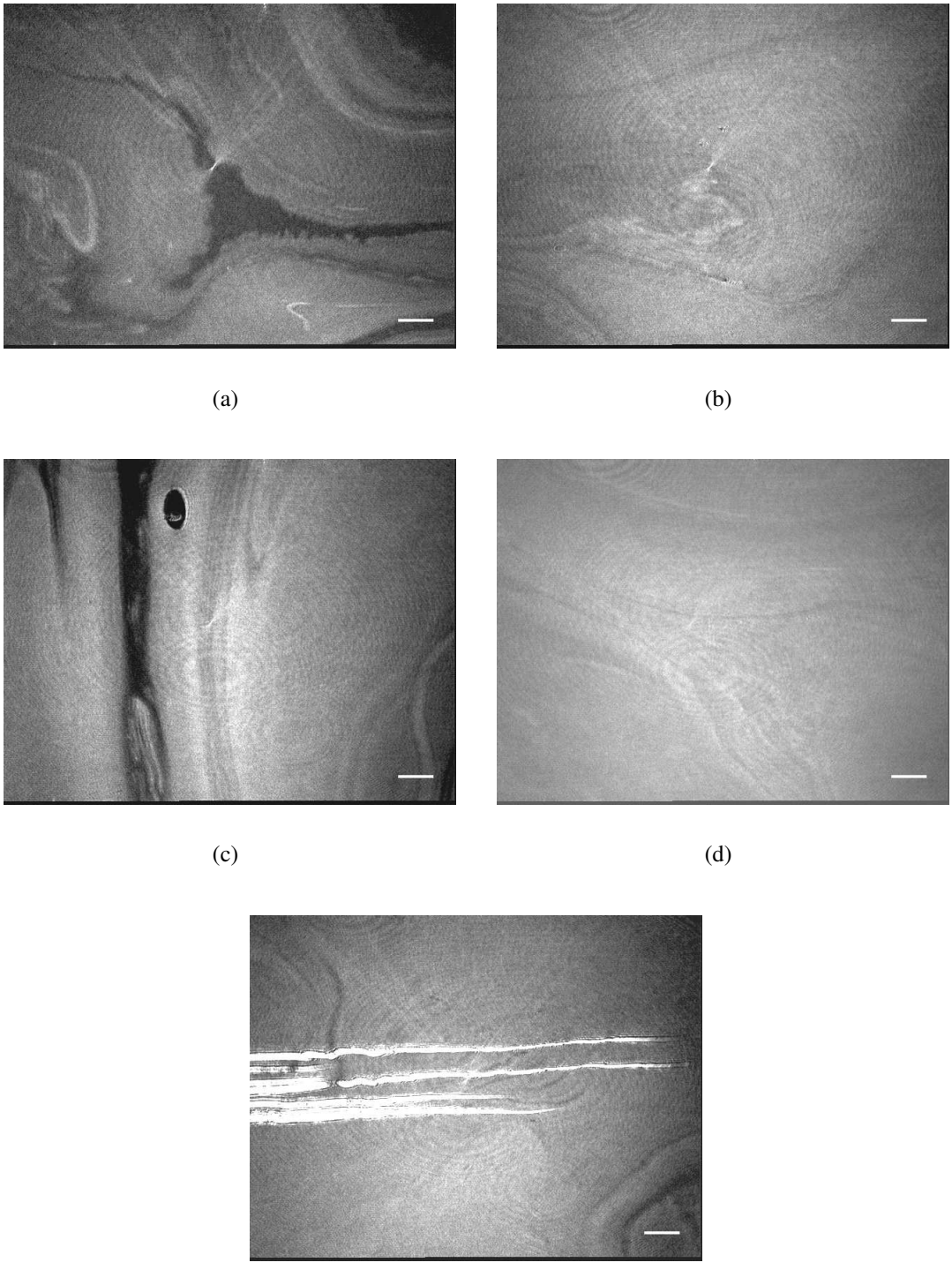

(a) (b)

(c) (d)

(e)

Figure 6.7: Brewster angle microscope images taken during compression of the TpImTp-DNA complex monolayer film at the air-water interface. (a) Coexistence of gas phase and expanded phase (A_m= 2.4 nm^2/molecule). (b) Expanded phase (A_m= 1.75 nm^2/molecule). (c) Coexistence of expanded and condensed phase (A_m= 1.4 nm ^{2}/molecule). (d) Condensed phase (A_m= 1.1 nm^2/molecule). (e) Collapsed state (A_m= 0.9 nm ^{2}/molecule). The scale bar in each image represents 500 μm.

6.3.3 Atomic Force Microscopy

The pure TpImTp monolayer was transferred at a target surface pressure (π_t) of 35 mN/m by Langmuir-Blodgett (LB) technique onto silicon substrates. Figure 6.8(a) shows the AFM topography image of the TpImTp LB film with one layer on hydrophilic silicon substrate. The film exhibited a uniform surface. The scratch made on the film with the AFM tip revealed a film height of about 2 nm. Figure 6.8(b) shows the AFM topography image of the TpImTp LB film with two layers on hydrophobic silicon substrate. The film showed a height of about 4 nm.

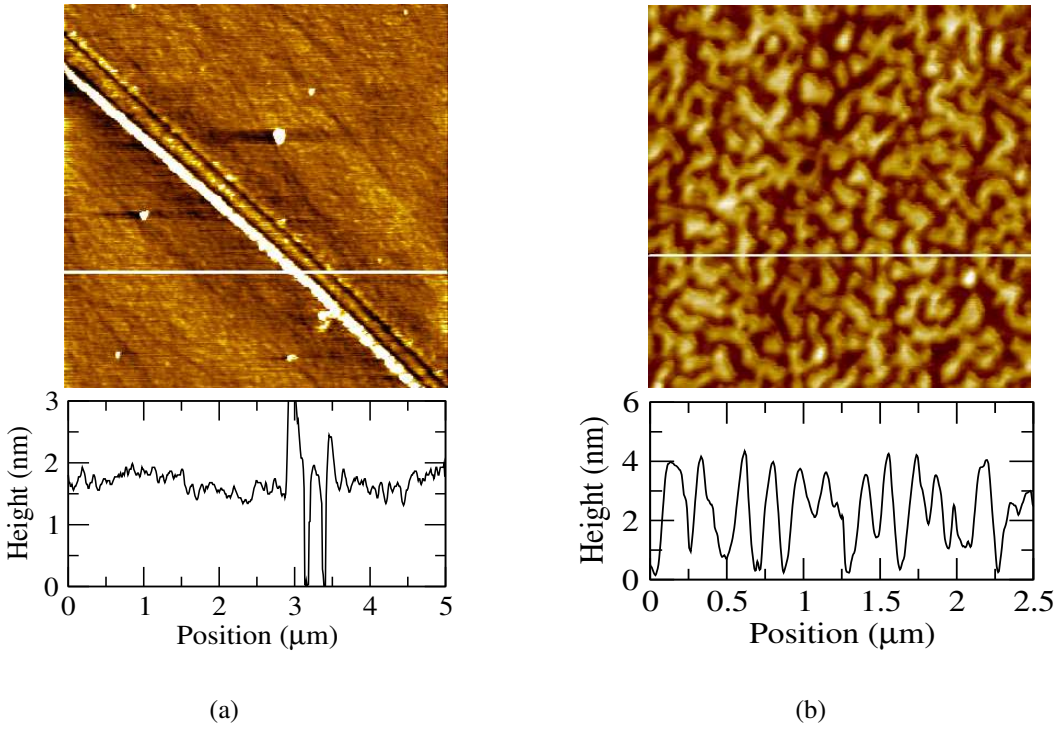

Figure 6.8: AFM topography images of pure TpImTp LB films transferred at π_t = 35 mN/m. (a)Film with 1 layer on hydrophilic silicon substrate. We have scratched the film with the AFM tip to find the height. (b)Film with 2 layers on hydrophobic silicon substrate. The respective height profiles corresponding to the lines drawn on the images are shown below.

The AFM topography images for the LB films of TpImTp with 4 and 8 layers are shown in Figures 6.9(a) and 6.9(b) respectively. The film surfaces were not uniform in both the cases. Hence, the line profiles drawn on the images do not correspond to the actual film heights. The films were scratched with an AFM tip to find the actual height. The scratching of the films revealed the film heights of about 8 nm for 4 layers and 16 nm for 8 layers as shown in Figures 6.9(c) and

6.9(d) respectively. Figures 6.10(a) and 6.10(b) show the topography of the LB films of the pure TpImTp with 15 layers on hydrophilic and 20 layers on hydrophobic silicon substrates. Both the films exhibited irregular surfaces and the heights revealed by the topography images do not correspond to the actual film heights. We have not scratched these films to find the actual height because the surface was very irregular and the thickness was high, which is likely to damage the AFM tip.

The TpImTp-DNA complex monolayer, on a subphase containing 10^{-8} M concentration of DNA, was transferred at different target surface pressures by LB technique. The AFM topography images of the TpImTp-DNA complex monolayer transferred at π_t values of 10 mN/m, 35 mN/m and 55 mN/m onto hydrophilic silicon substrates are shown in Figure 6.11. The film transferred at 10 mN/m was not compact and showed a height of about 0.5 nm (Figure 6.11(a)). The film transferred at 35 mN/m was compact (Figure 6.11(b)). This compact film was scratched with AFM tip. The height profile revealed a height of about 2.2 nm with respect to the scratched area on the film (Figure 6.11(c)). The film transferred at 55 mN/m (Figure 6.11(d)) showed thread-like domains in the collapsed state which were also observed in the BAM images.

The AFM topography images of TpImTp-DNA complex LB films with 2 and 4 layers transferred onto hydrophobic silicon substrates are shown in Figures 6.12(a) and 6.12(b) respectively. The height profile revealed by the topography does not correspond to the actual film height. Hence, the films were scratched with an AFM tip to find the actual height. Figures 6.12(c) and 6.12(d) show the scratched films with 2 and 4 layers respectively. The heights of about 4 nm for the film with 2 layers and about 8 nm for the film with 4 layers were obtained with reference to the scratched area on the films.

We have transferred the TpImTp-DNA complex films upto 20 layers. Figures 6.13(a) and 6.13(b) show the complex film with 8 and 20 layers transferred onto hydrophobic silicon substrates at π_t of 35 mN/m. The TpImTp-DNA complex films were scratched with AFM tip to find the actual film heights. We obtained film heights of about 16 nm and 40 nm with reference to the scratched area for the films with 8 and 20 layers respectively (Figures 6.13(c) and 6.13(d)). It is to be noted that the film heights obtained for these multilayer TpImTp-DNA complex films were close

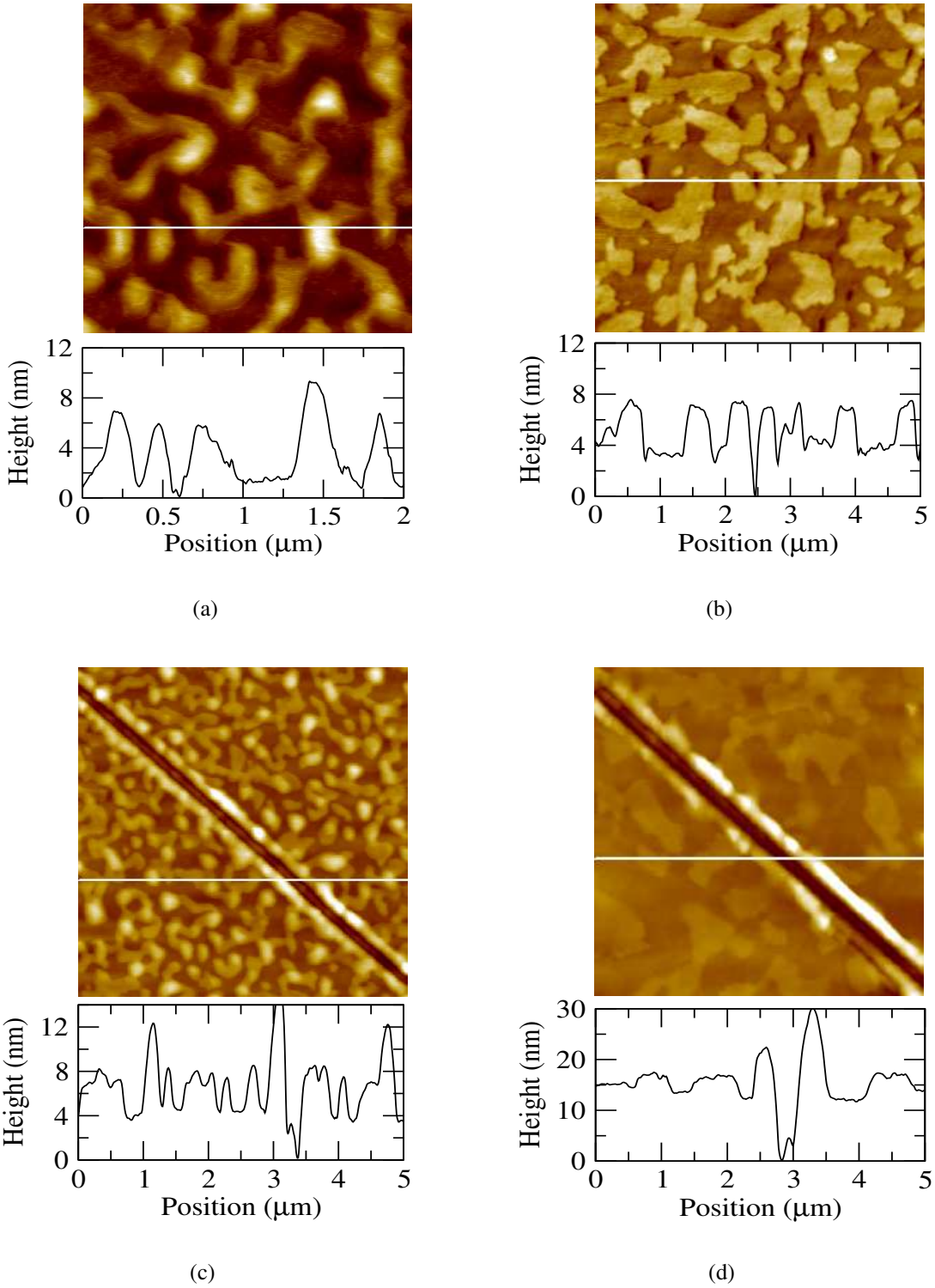

Figure 6.9: AFM topography images of pure TpImTp LB films with (a) 4 layers and (b) 8 layers, transferred onto hydrophobic silicon substrates at π_t = 35 mN/m. The films are scratched with the AFM tip to find the actual height. (c) Scratched film with 4 layers. (d) Scratched film with 8 layers. The respective height profiles corresponding to the lines drawn on the images are shown below.

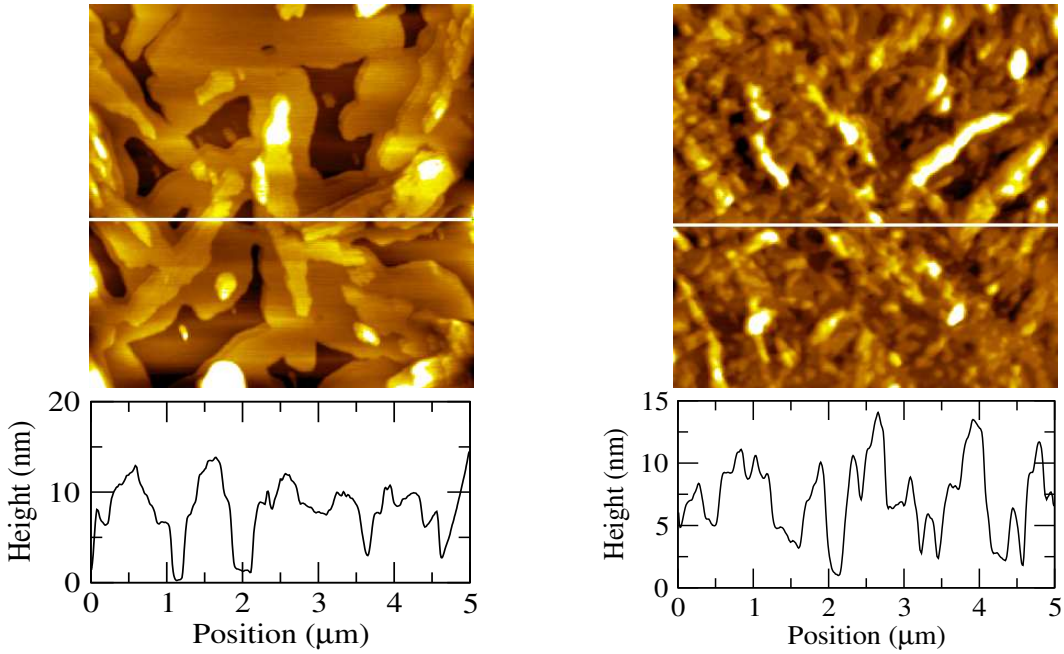

(a) (b)

Figure 6.10: AFM topography images of pure TpImTp LB films with (a) 15 layers transferred onto hydrophilic silicon substrate and (b) 20 layers transferred onto hydrophobic silicon substrate, at π_t = 35 mN/m. The respective height profiles corresponding to the lines on the images are shown below.

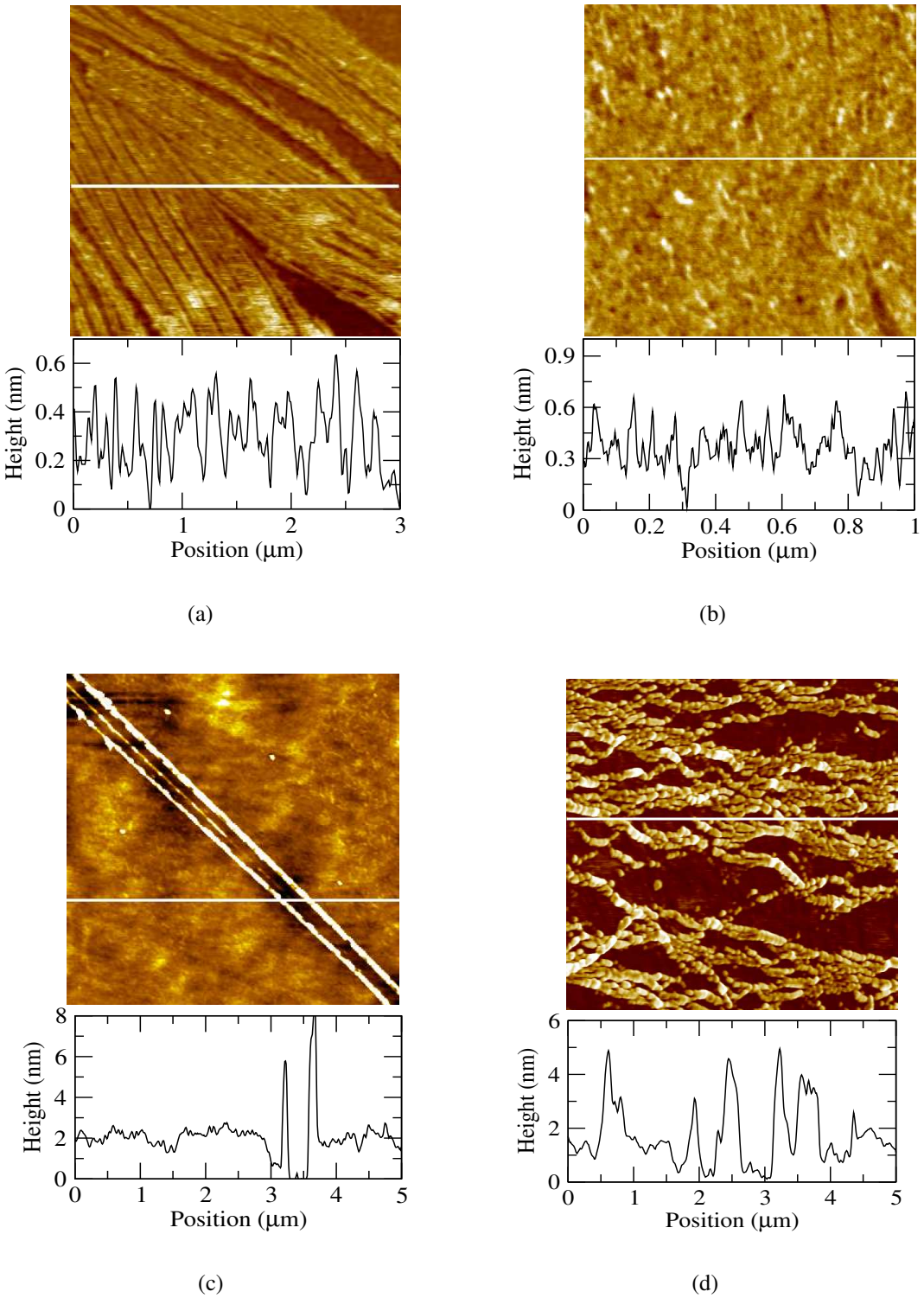

Figure 6.11: AFM topography images of TpImTp-DNA complex LB films with one layer transferred onto hydrophilic silicon substrate at different target surface pressures. (a) π_t = 10 mN/m; expanded phase. (b) π_t = 35 mN/m; condensed phase. (c) The film in the condensed phase transferred at π_t = 35 mN/m is scratched to find the film height. (d) π_t = 55 mN/m; collapsed state. The respective height profiles corresponding to the lines drawn on the images are shown below.

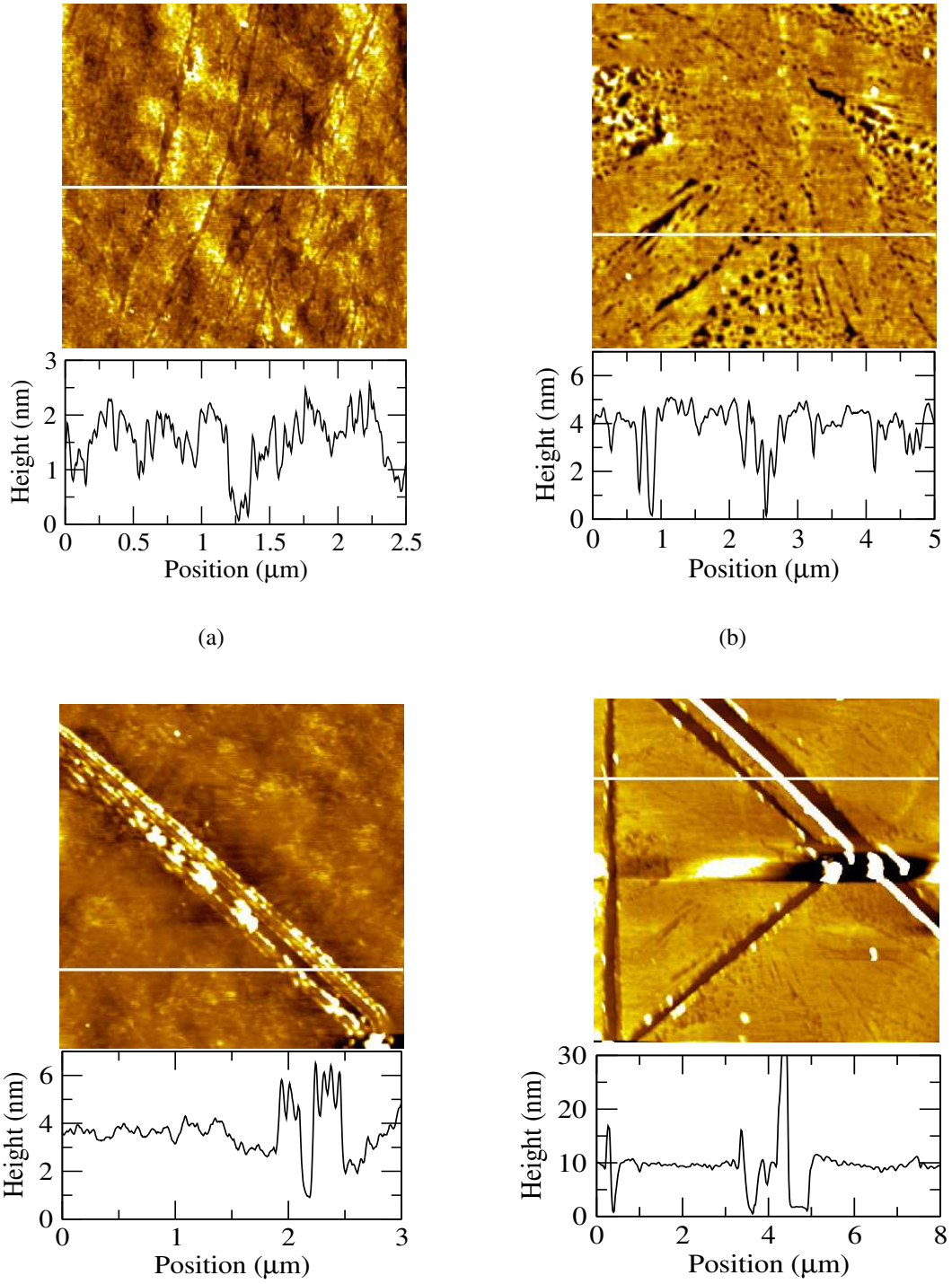

Figure 6.12: AFM topography of TpImTp-DNA complex LB films with (a) 2 layers and (b) 4 layers transferred onto hydrophobic silicon substrates at π_t = 35 mN/m. The films are scratched with AFM tip to find the actual height. (c) Scratched film with 2 layers. (d) Scratched film with 4 layers. The respective height profiles corresponding to the white line on the images are shown below.

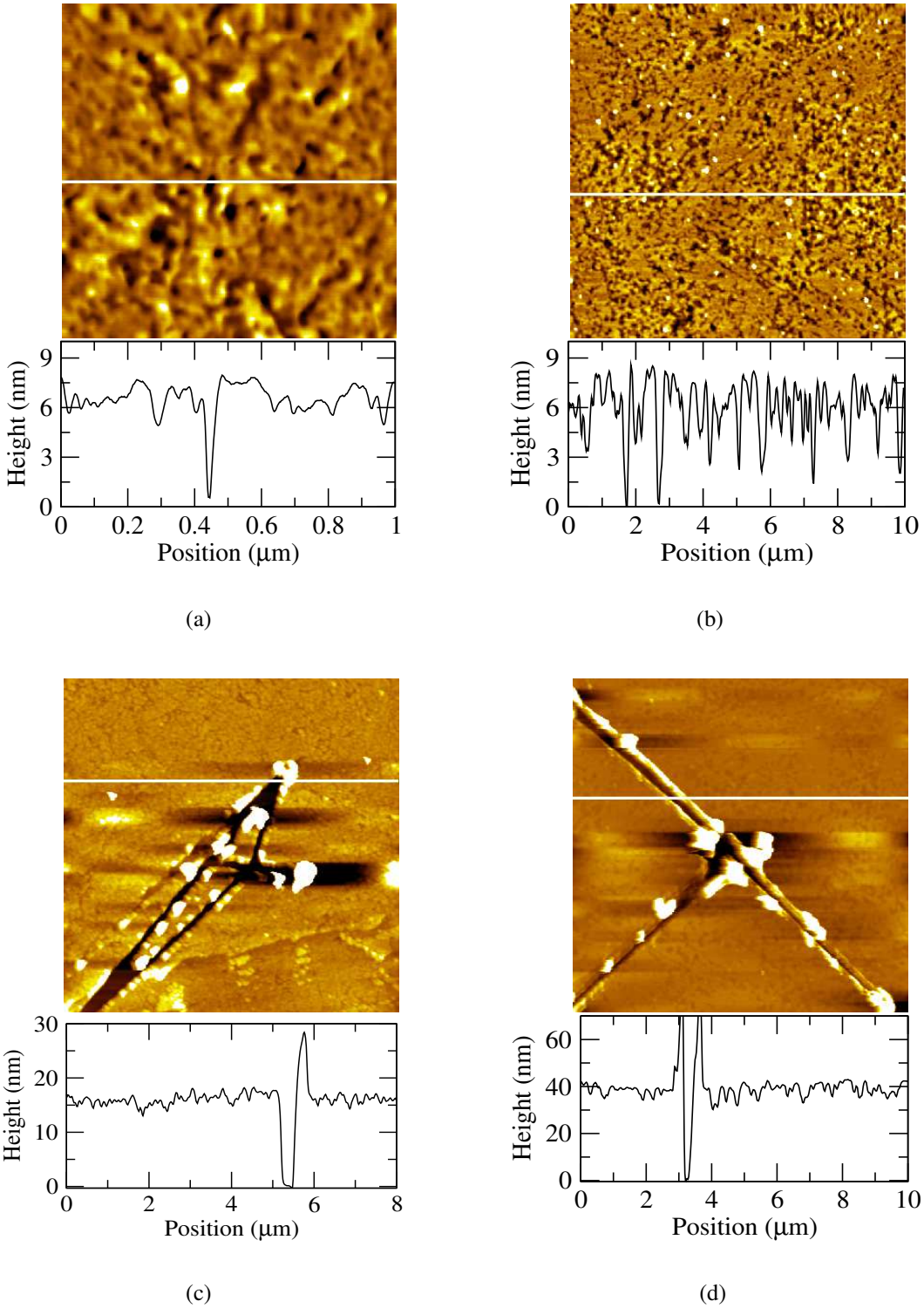

Figure 6.13: AFM topography of TpImTp-DNA complex LB films with (a) 8 layers and (b) 20 layers transferred onto hydrophobic silicon substrates at π_t = 35 mN/m. The films are scratched with AFM tip to find the actual height. (c) Scratched film with 8 layers. (d) Scratched film with 20 layers. The respective height profiles corresponding to the white line on the images are shown below.

to those expected for the pure TpImTp multilayer films. Also, we did not observe any thread-like structures in the multilayer films of the TpImTp-DNA complex as in the case of multilayer films of PyTp-DNA complex [18] presented in Chapter 3.

In addition, we have transferred the film of monomer ImTp-DNA complex onto silicon substrates by LB technique. The film, formed on a subphase containing 10^{-7} M concentration of DNA, was transferred at a target surface pressure of 35 mN/m. The topography of these LB films showed similar features as that of the dimer TpImTp-DNA complex film. Figure 6.14 shows AFM topography images of ImTp-DNA complex LB film with 20 layers transferred onto hydrophobic silicon substrate. The surface of this film was very rough. Similar to the dimer TpImTp-DNA complex multilayer film, the monomer ImTp-DNA complex film also did not show any thread-like structure.

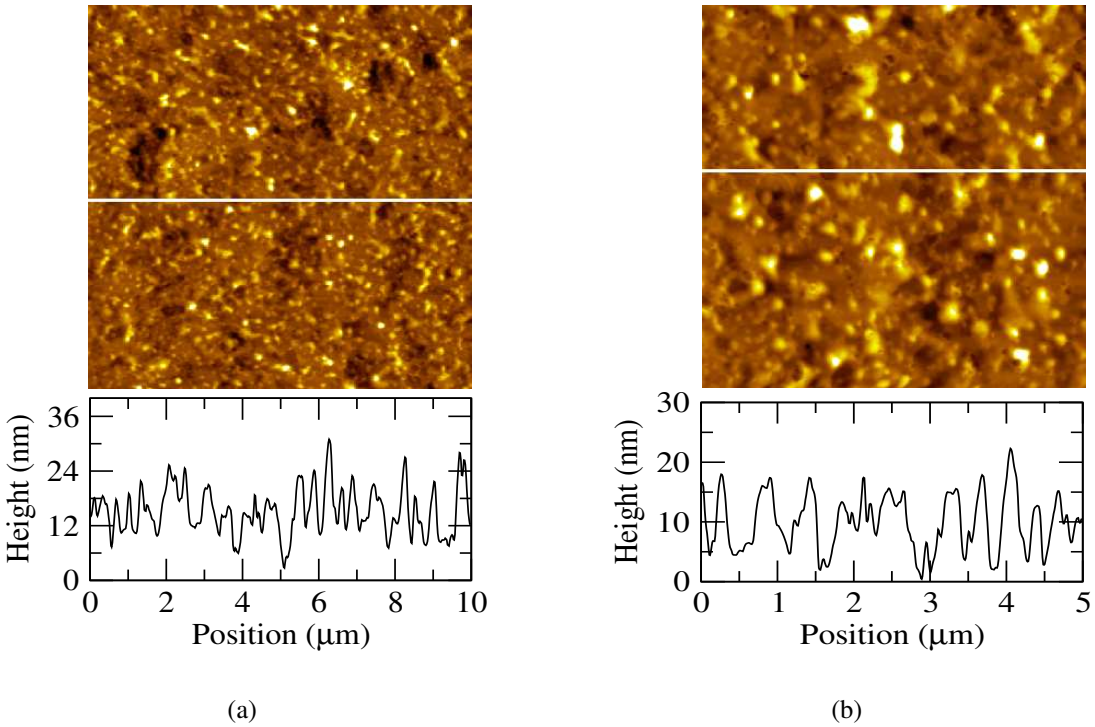

Figure 6.14: AFM topography images of ImTp-DNA complex LB film with 20 layers on hydrophobic silicon substrate. (a) $10 \times 10\ \mu m^2$. (b) $5 \times 5\ \mu m^2$. The respective height profiles corresponding to the white line on the images are shown below.

6.3.4 Transfer Ratios of the LB Films

We have measured the transfer ratios of the LB films of the pure TpImTp dimer monolayer. The transfer ratio (τ) data of the LB films of the pure TpImTp with 15 layers on hydrophilic silicon substrate and 20 layers on hydrophobic silicon substrate transferred at a target surface pressure (π_t) of 35 mN/m are shown in Figures 6.15(a) and 6.15(b) respectively. For the hydrophilic silicon substrate, there was alternate desorption and adsorption after the first two layers of deposition. The desorption was less compared to the adsorption leading to some deposition of the material onto the substrate over successive deposition cycles. For hydrophobic silicon substrate, the transfer was efficient only for the first few layers. In the successive strokes of deposition, the transfer efficiency was found to decrease significantly. Thus, for the pure TpImTp dimer film, multilayer formation was not very efficient on both hydrophilic and hydrophobic silicon substrates.

When the TpImTp film was complexed with DNA (10^{-8} M concentration in the subphase), the transfer efficiency increased drastically. Figures 6.16(a) and 6.16(b) show the τ data for the TpImTp-DNA complex film transferred at a π_t of 35 mN/m on hydrophilic and hydrophobic silicon substrates respectively. On hydrophilic silicon substrate, the τ value was around 1 for every upstroke of film deposition even upto 40 layers (Figure 6.16(a)). The τ value was found slightly less (ranging between 0.9 to 0.6) for every downstroke of film deposition. This difference in the value of τ for the upstrokes and downstrokes may be attributed to the difference in the flow pattern of the subphase near the meniscus region during the up and downstrokes of LB deposition [19]. Interestingly, we find that on hydrophobic silicon substrate, the τ value was around 1 for both the upstroke and downstroke of film deposition (Figure 6.16(b)). This deposition continued with the same efficiency even upto 20 layers. Thus, although we could deposit multilayers of TpImTp-DNA complex film on both the hydrophilic and hydrophobic silicon substrates efficiently, we note that on hydrophobic silicon substrate the deposition was remarkably perfect.

In addition, we have measured the transfer ratio of LB films of the monomer ImTp-DNA complex. The τ data for the ImTp-DNA complex film transferred at a π_t of 35 mN/m on hydrophobic silicon substrate is shown in Figure 6.17. This film showed poor deposition after the first two layers. The successive upstrokes showed good deposition ($\tau \sim 1$) whereas the down strokes

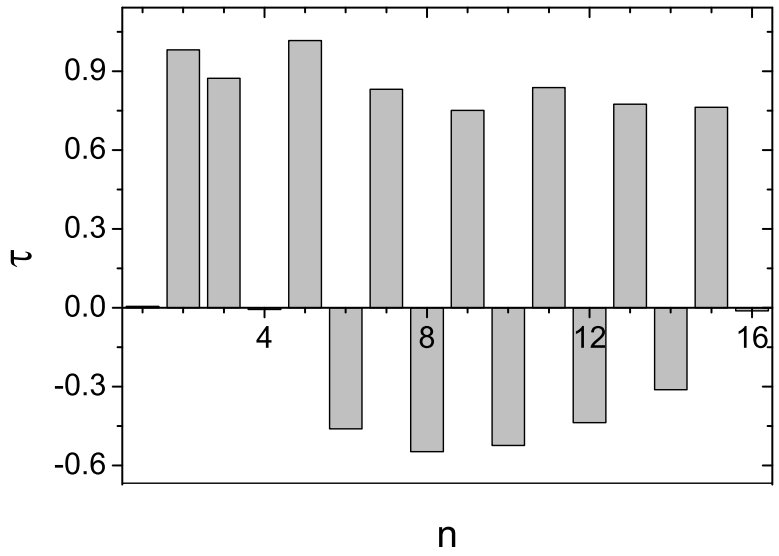

(a)

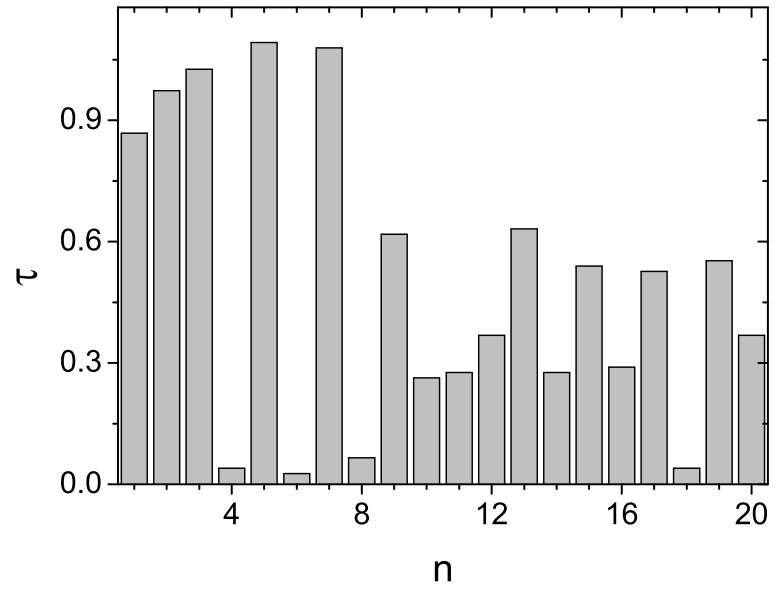

(b)

Figure 6.15: Transfer ratio (τ) as a function of number of layers (n) of LB film deposition for TpImTp on (a) hydrophilic and (b) hydrophobic silicon substrates. The film was transferred at a target surface pressure of 35 mN/m and a dipping speed of 2 mm/min.

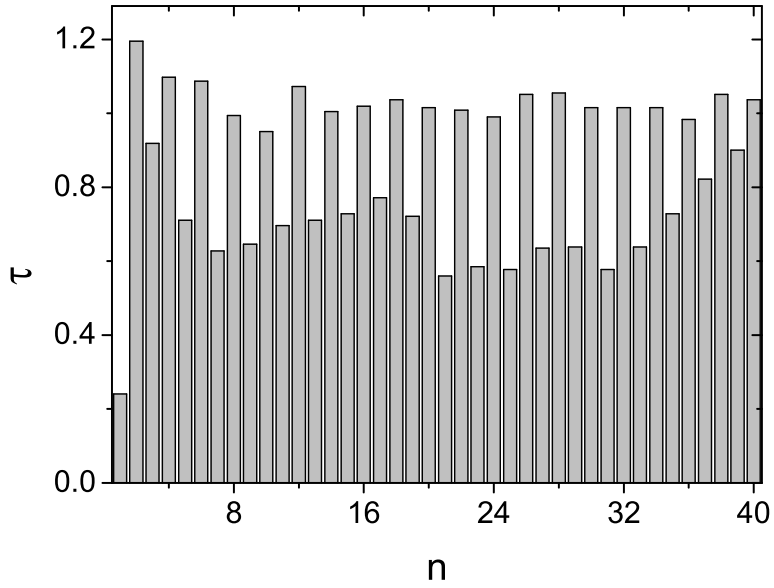

(a)

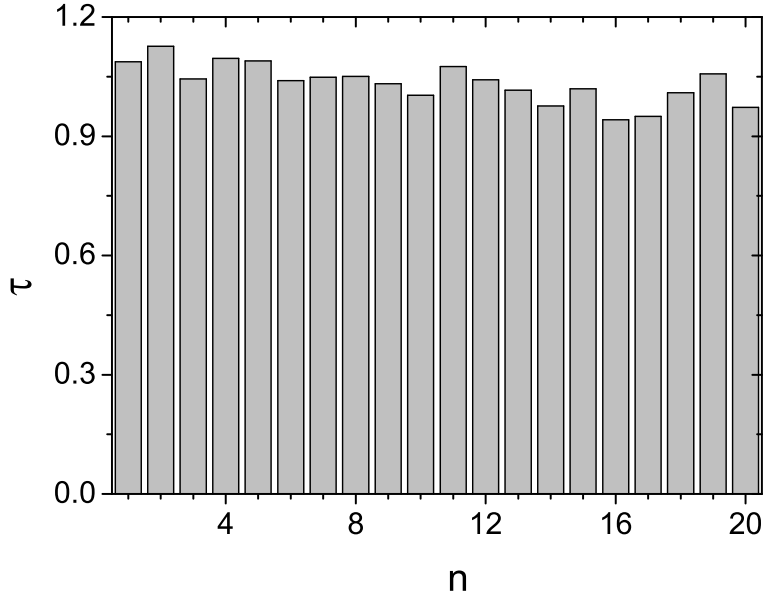

(b)

Figure 6.16: Transfer ratio (τ) as a function of number of layers (n) of LB film deposition for TpImTp-DNA complex on (a) hydrophilic and (b) hydrophobic silicon substrates. The film was transferred at a target surface pressure of 35 mN/m and a dipping speed of 2 mm/min.

showed either desorption or less deposition. Our measurement of transfer ratio of the ImTp-DNA complex film on hydrophobic silicon substrate showed even more inefficient deposition compared to hydrophobic silicon substrate. Under these situations, although we could form multilayer of the monomer ImTp-DNA complex film, it was not very efficient unlike the multilayer of dimer TpImTp-DNA complex film.

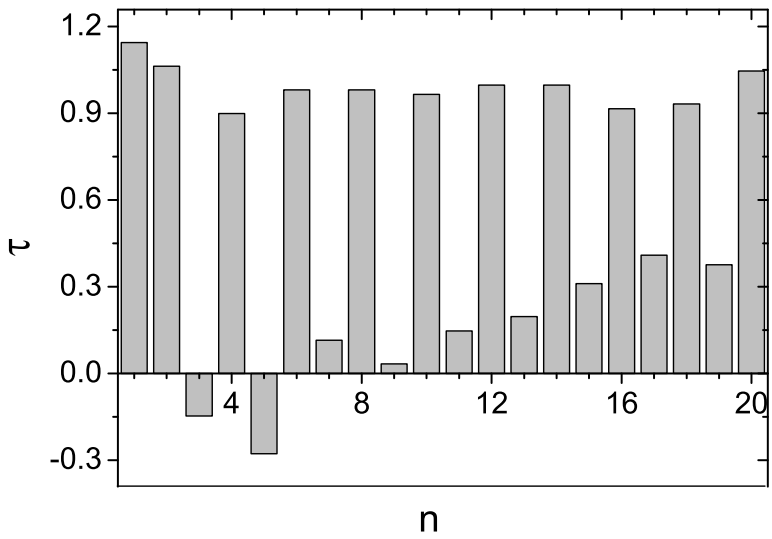

Figure 6.17: Transfer ratio (τ) as a function of number of layers (n) of LB film deposition for ImTp-DNA complex on hydrophobic silicon substrate. The film was transferred at a target surface pressure of 35 mN/m and a dipping speed of 2 mm/min.

6.4 Discussion

The surface pressure (π) - area per molecule (A_m) isotherm for the pure TpImTp molecule (Figure 6.1) showed single phase with a limiting area (A_o) of 1.97 nm^2/molecule. The compressional elastic modulus (|E|) value calculated for this phase was 132.3 mN/m. The isotherm of TpImTp-DNA complex with 10^{-8} M concentration of DNA in the subphase (Figure 6.3) showed two distinct phases with A_o values of 2.2 and 1.56 nm^2/molecule. The |E| values calculated for these two phases were 24 and 163 mN/m (Figure 6.4). On the basis of these |E| values, we suggest that the pure TpImTp monolayer exhibits a condensed phase, whereas, the TpImTp-DNA complex monolayer

undergoes a transformation from an expanded phase to a condensed phase. In addition, we find that the A_o value corresponding to the condensed phase of the complex film is much less than that of the pure film. This indicates that the presence of DNA in the subphase condenses the TpImTp monolayer film. The isotherm cycle of TpImTp (Figure 6.2) showed negligible hysteresis indicating a reversible collapse. Under BAM, it was observed that the collapsed domains reverted back to monolayer state on expansion (Figure 6.6). This observation confirms the reversible collapse of TpImTp monolayer. On the other hand, BAM studies on the TpImTp-DNA complex monolayer showed that the collapse state was irreversible (Figure 6.7).

We would like to remark that the surface manometry studies showed 10^{-8} M concentration of DNA in the subphase to be the optimum condition for the formation of a stable complex monolayer at the air-water interface. We find that adding DNA in the subphase more than this concentration did not further alter the monolayer properties at the air-water interface. This was true for all the three ionic discotic molecules studied so far, viz., PyTp, ImTp and TpImTp.

In Chapter 2, we have presented the surface manometry studies of the ImTp molecule [15]. The ImTp molecule is the monomeric analog of the TpImTp dimer molecule and hence it is interesting to compare their results. From their isotherms, we find that the dimer exhibited comparatively more A_o value than that of the monomer. This is quite reasonable since the dimer has bigger dimension compared to the monomer molecule. Interestingly, we find that the |E| value calculated from the isotherm of the dimer is 2.4 times greater than that of the monomer. This indicates that the packing of molecules in the monolayer of dimer is better than that of its monomer. It is known in literature that the packing of discotic mesogens is predominantly governed by the π-π interaction between the cores [4]. In our system, the TpImTp dimer molecule consist of two triphenylene cores. Due to this, there are more delocalized π electrons in TpImTp dimer molecule than that of the monomeric ImTp molecule. Hence, there is a possibility of a greater degree of π-π interaction between the adjacent cores. This leads to a better packing of TpImTp molecules in the monolayer at the air-water interface as compared to its monomer analog. Consequently, the TpImTp-DNA complex monolayer film also showed much greater |E| value (163 mN/m) than that of the ImTp-DNA complex monolayer film (98 mN/m) as shown in Figures 6.4 and 6.5 respectively.

The AFM studies provide information about the organization of the TpImTp molecules on a solid substrate. The topography image of single layer of TpImTp monolayer film transferred at the condensed phase (35 mN/m) showed a uniform film with a height of about 2 nm (Figure 6.8(a)). From the surface manometry studies, we have obtained A_0 value of 1.97 nm^2/molecule for the condensed phase. Comparing the film height and the A_o value with the molecular dimensions, we suggest that this condensed phase is composed of molecules arranged in an edge-on configuration. We have represented in Figure 6.18 the schematic diagram of the possible configurations of TpImTp molecules on a surface, and estimated the A_o values based on molecular dimensions. For a face-on configuration, the estimated A_o value is 8.6 nm^2/molecule (Figure 6.18(a)), whereas for an edge-on arrangement, the estimated A_o value is 1.46 nm^2/molecule (Figure 6.18(b)). It is to be noted that the A_o value obtained from the surface manometry measurements was larger than the theoretically estimated value for the edge-on arrangement. This may be attributed to the electrostatic repulsion between the molecules in the monolayer since the molecules are charged. Also, we note that, unlike the monomeric ImTp film [15], the TpImTp film does not exhibit a face-on configuration.

Further, we have transferred these films onto silicon substrates by LB technique. We have studied the topography and thickness of these LB films using an AFM. The AFM images of the LB films of pure TpImTp with 2, 4 and 8 layers (Figures 6.8(b) and 6.9) show irregular morphology. This may be attributed to several factors like reorganization of molecules in the film during the transfer process, natural dewetting of the film, evaporation of entrapped water within the layers and varying transfer efficiency for different layers of deposition [20, 21]. With hydrophilic silicon substrate, we observed desorption of the film back to the subphase for the successive up strokes (Figure 6.15(a)). The deposition was comparatively better on a hydrophobic substrate and there was no desorption. But the efficiency of transfer decreased drastically for higher number of layers (Figure 6.15(b)). Hence, good multilayer film deposition of pure TpImTp was not possible on either hydrophilic or hydrophobic silicon substrates. This is also confirmed by the irregular heights shown by the topography images of LB films with 15 and 20 layers (Figure 6.10).

The topography images of the TpImTp-DNA complex LB film with single layer transferred in

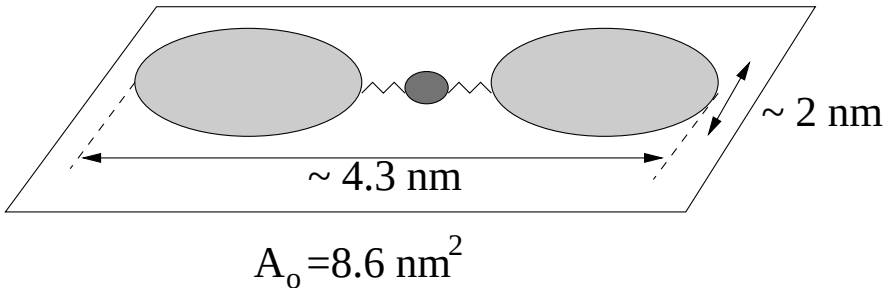

(a)

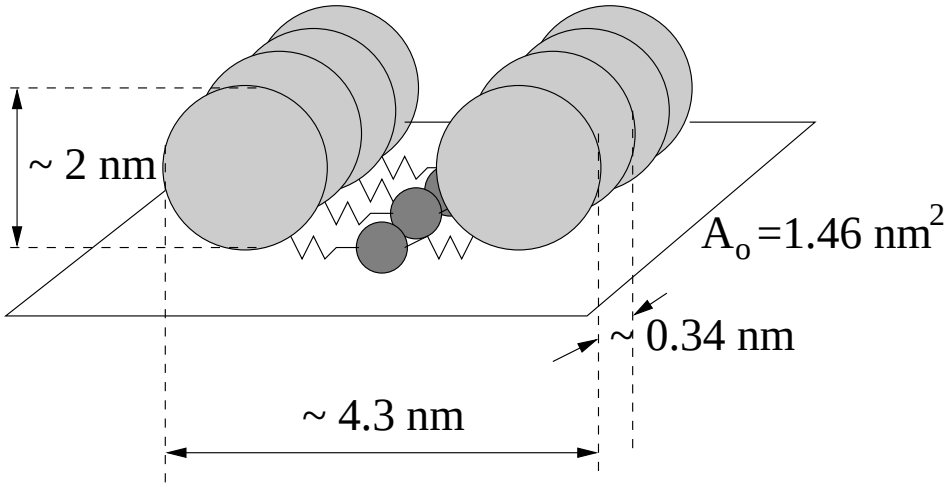

(b)

Figure 6.18: Schematic diagram of the possible arrangements of TpImTp molecules on a surface. (a) Face-on. (b) Edge-on, here the intracolumnar core to core distance of 0.34 nm is taken from reference 10. The A_o values are estimated based on the molecular dimensions.

the expanded phase shows a height of about 0.5 nm, and in the condensed phase shows a height of about 2.2 nm (Figures 6.11(a) and 6.11(c)). From the surface manometry studies we have obtained A_0 values of 2.2 nm^2/molecule for the expanded phase and 1.56 nm^2/molecule for the condensed phase. An estimated dimension of the TpImTp dimer compactly packed in the edge-on configuration yields a value of A_0 to be 1.46 nm^2 (Figure 6.18(b)). Comparing this value with the A_0 values for TpImTp-DNA complex film obtained from surface manometry and the film heights obtained from AFM studies, we suggest that the expanded phase is composed of loosely packed molecules in an edge-on configuration and the condensed phase is composed of densely packed molecules in an edge-on configuration. In Figure 6.19, we schematically represent the edge-on configuration of TpImTp molecules at the A-W interface with DNA in the subphase.

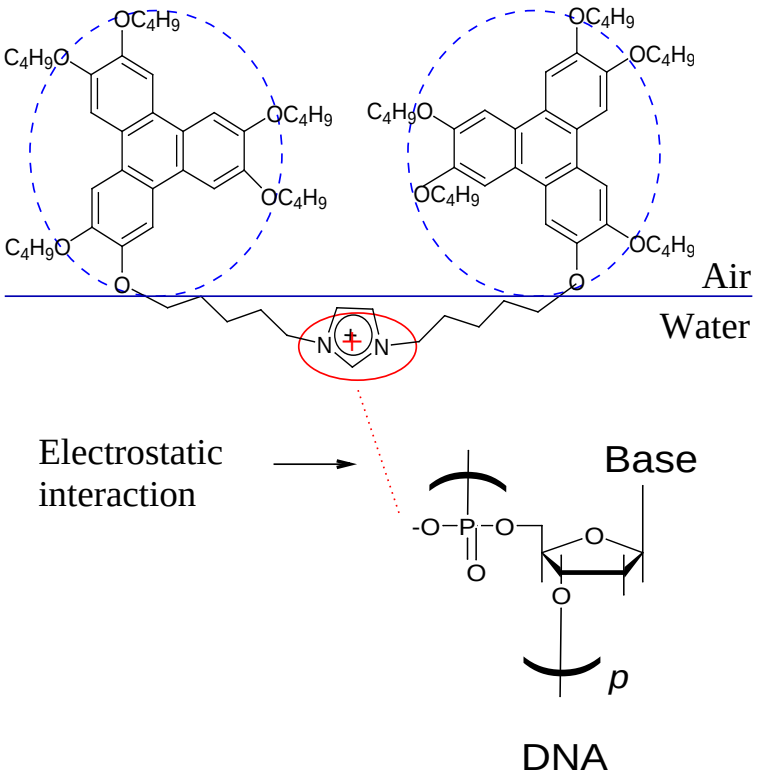

Figure 6.19: Schematic representation of the edge-on configuration of the TpImTp-DNA complex monolayer at the air-water interface.

Further, we have studied the topography of the TpImTp-DNA complex films with 2, 4, 8 and 20 layers transferred onto hydrophobic silicon substrates at a target surface pressure of 35 mN/m (Figures 6.12 and 6.13). The heights obtained by scratching the films with the AFM tip were

4, 8, 16 and 40 nm for the TpImTp-DNA complex film with 2, 4, 8 and 20 layers respectively. Interestingly, this gives a thickness of 2 nm for each layer of successive deposition. It is to be noted that these film heights also correspond to those expected for the pure TpImTp film with the similar number of layers. This indicates that sufficient DNA molecules do not get transferred to the substrate to form DNA bundles as found in PyTp-DNA complex films [22]. However, the formation of multilayers with almost perfect transfer ratio indicates that DNA does play a role. We also do not find the extra thickness of 1 nm and the formation of thread-like structures. In addition, our Fourier transform infrared (FTIR) spectroscopy of the TpImTp-DNA complex LB film did not indicate prominent characteristic absorption bands of a DNA molecule. These observations suggest that very few DNA molecules get transferred onto substrates in the process of LB film deposition, but they help to form a film with full coverage.

In addition, we have transferred the monomer ImTp-DNA complex film on silicon substrates and studied them using AFM (Figure 6.14). The ImTp-DNA complex multilayer LB films showed features similar to that of the dimer TpImTp-DNA complex film, i.e., thread-like structures were absent and there was no increase in film thickness. Here again, the FTIR spectroscopy of these films did not show any prominent absorption band of DNA. On the basis of all these observations, we suggest that the interaction of the monomer ImTp as well as the dimer TpImTp with DNA is not strong enough to lift DNA molecules from the air-water to the air-solid interface.

It appears that the cationic polar head groups plays a significant role in the transfer of DNA onto substrates. For the PyTp molecule, the polar head group is a pyridinium moiety. In a pyridine moiety, the replacement of a CH in the benzene ring by more electronegative nitrogen atom induces a dipole moment of 2.2 D, denoting a shift of electron density from the ring towards the nitrogen atom [23, 24]. (Benzene molecule which is symmetrical has zero dipole moment.) For ImTp and TpImTp molecules, the polar head group is a imidazolium moiety. In an imidazole moiety, the replacement of CH by electronegative nitrogen atom at two positions, induces a dipole moment of 3.61 D. The valence bond (resonance) description indicates that both the pyridinium ring and the imidazolium ring have delocalized positive charge [25]. An important point to note is that one of the nitrogen atoms of imidazolium moiety carries a lone pair of electrons. These electrons are not

part of the π-system. Hence, they tend to screen the effective positive charge of the imidazolium ring. The complex formation with DNA is primarily an electrostatic interaction. The screening of the effective positive charge on imidazolium ring reduces the strength of electrostatic interaction with negatively charged DNA molecules. This might be a possible reason for the inability of ImTp and TpImTp monolayers to transfer large number of DNA molecules from the air-water to the air-solid interface.

Another possible reason might be due to the steric hindrance. The ImTp molecule has an extra methyl group attached to one of the nitrogen atoms of the ring which causes steric hindrance. The TpImTp molecule, which is a dimer, also has a pronounced effect of steric hindrance [2]. Such an effect may cause hindrance to the DNA binding, thereby affecting its transfer onto substrates in the process of LB deposition.

6.5 Conclusions

The novel ionic discotic dimer (TpImTp) exhibited stable Langmuir monolayer. The collapsed state of the TpImTp film completely reverted to the monolayer state on expansion. As compared to its monomer analog, the TpImTp monolayer exhibited higher compressional elastic modulus, indicating a much better packing of molecules in the monolayer. This is probably due to the two aromatic cores in a TpImTp molecule which enhances the π-stacking interaction. The complexation of the TpImTp monolayer with DNA at air-water interface results in a decrease in limiting area and an increase in the collapse pressure. In addition, DNA complexation facilitated the extremely efficient (transfer ratio ~ 1) multilayer formation of the TpImTp monolayer on a substrate. However, the TpImTp-DNA complex could not transfer large number of DNA molecules from the air-water to the air-solid interface efficiently. This may be attributed to the fact that the lone pair of electrons on one of the nitrogen atoms in imidazolium moiety screen the effective positive charge of the ring, thereby decreasing the strength of electrostatic interaction with DNA. In addition, the steric hindrance may play a significant role particularly in case of bulky groups like dimers.

Upto this chapter, we have dealt with discotic molecules which have ionic polar groups. We have studied their organization at the air-water and the air-solid interfaces. It is to be noted that all these ionic systems share a common feature. The LB deposition was inefficient for these ionic systems and the efficiency drastically improved by adding DNA in the subphase. In literature, it is known that the deposition of charged Langmuir monolayer on a substrate by LB method involves complicated physical and chemical processes [21]. It would be interesting to study a non-ionic discotic system so that we can have a direct comparison between the properties exhibited by an ionic discotic system and a non-ionic discotic system at interfaces. In the next chapter, we present our studies on a non-ionic discotic molecule to explore how the absence of an ionic polar group affects the properties of Langmuir monolayer and LB films.

Bibliography

[1] S. Sergeyev, W. Pisula, and Y. H. Geerts, *Chem. Soc. Rev.* **36**, 1902 (2007).

[2] Sandeep Kumar, *Liq. Cryst.* **32**, 1089 (2005).

[3] W. Kreuder, H. Ringsdorf, O. H. Schonherr, and J. H. Wendorff, *Angew. Chem. Int. Ed.* **26**, 1249 (1987).

[4] Sandeep Kumar, *Chem. Soc. Rev.* **35**, 83 (2006).

[5] S. Ito, P. T. Herwig, T. Bohme, J. P. Rabe, W. Rettig, and K. Mullen, *J. Am. Chem. Soc.* **122**, 7698 (2000).

[6] L. Zhi, J. Wu, and K. Mullen, *Org. Lett.* **7**, 5761 (2005).

[7] M. D. Watson, F. Jackel, N. Severin, J. P. Rabe, and K. Mullen, *J. Am. Chem. Soc.* **126**, 1402 (2004).

[8] K. Hatsusaka, N. Kimura, and K. Ohta, *Bull. Chem. Soc. Jpn.* **76**, 781 (2003).

[9] N. C. Maliszewskyj, P. A. Heiney, J. Y. Josefowicz, T. Plesnivy, H. Ringsdorf, and P. Schuhmacher, *Langmuir* **11**, 1666 (1995).

[10] V. V. Tsukruk, H. Bengs, and H. Ringsdorf, *Langmuir* **12**, 754 (1996).

[11] V. V. Tsukruk and D. Janietz, *Langmuir* **12**, 2825 (1996).

[12] A. Corma and H. Garcia, *Chem. Rev.* **103**, 4307 (2003).

[13] N. Yamanaka, R. Kawano, W. Kubo, T. Kitamura, Y. Wada, M. Watanabe, and S. Yanagida, *Chem. Commun.*, 740 (2005).

[14] M. Yoshio, T. Kagata, K. Hoshino, T. Mukai, H. Ohno, and T. Kato, *J. Am. Chem. Soc.* **128**, 5570 (2006).

[15] Alpana Nayak, K. A. Suresh, Santanu Kumar Pal, and Sandeep Kumar, *J. Phys. Chem. B* **111**, 11157 (2007).

[16] Santanu Kumar Pal and Sandeep Kumar, *Tetrahedron Letters* **47**, 8993 (2006).

[17] J. T. Davies and E. K. Rideal, *Interfacial Phenomena*; Academic Press: New York, 1961.

[18] Alpana Nayak and K. A. Suresh, *J. Phys. Chem. B* **112**, 2930, (2008).

[19] M. Elena Diaz and R. L. Cerro, *Thin Solid Films* **460**, 274 (2004).

[20] H. D. Sikes, J. T. Woodward IV, and D. K. Schwartz, *J. Phys. Chem.* **100**, 9093 (1996).

[21] V. I. Kovalchuk and D. Vollhardt, *Adv. Colloid Interface Sci.* **114-115**, 267 (2005).

[22] Alpana Nayak and K. A. Suresh, *Phys. Rev. E* **78**, 021606 (2008).

[23] B. A. Middleton and J. R. Partington, *Nature* **141**, 516 (1938).

[24] B. B. DeMore, W. S. Wilcox, and J. H. Goldstein, *J. Chem. Phys.* **22**, 876 (1954).

[25] M. Sainsbury, *Heterocyclic Chemistry*; Royal Society of Chemistry: Great Britain, 2001.